Multichip LED Modules With V-Groove Surfaces for Light Extraction Efficiency Enhancements Considering Roughness Scattering

Article *in* IEEE Transactions on Electron Devices · November 2016

DOI: 10.1109/TED.2016.2628788

CITATIONS
2

READS
216

6 authors, including:

Xinrui Ding
University of California, Berkeley
32 PUBLICATIONS **156** CITATIONS
SEE PROFILE

Zongtao Li
South China University of Technology
60 PUBLICATIONS **437** CITATIONS
SEE PROFILE

Jia-Sheng Li
South China University of Technology
15 PUBLICATIONS **51** CITATIONS
SEE PROFILE

Multichip LED Modules With V-Groove Surfaces for Light Extraction Efficiency Enhancements Considering Roughness Scattering

Xinrui Ding, Yong Tang, Zongtao Li, Jiasheng Li, Yingxi Xie, and Liwei Lin

***Abstract*— Although multichip light-emitting diode (LED) modules are becoming popular in high-power lighting applications, better light extraction efficiency is always desirable in the industry. In this paper, V-grooves fabricated by the low-cost dicing process have been utilized on the top face of the multichip LED module to enhance the output power. An analytical model including the consideration of surface has been established by using a fractal theory. The combined finite difference time domain and ray tracing method has been used to simulate the light extraction enhancement considering the surface roughness scattering effects. The results show 12% enhancements in the experiments when the measured surface roughness of the V-groove has RMS roughness of 0.25 μm, which is in good agreement with the simulation result of 13.7%. The multichip LED models have been applied in indoor downlight systems and it is found that the luminous efficiency has been enhanced by 9.6% under a current of 350 mA (5.8 W) when compared with multichip LED modules without V-grooves.**

***Index Terms*— Finite domain time difference (FDTD), multichip light-emitting diodes (LEDs), ray tracing (RT), surface roughness scattering.**

I. Introduction

LIGHT-EMITTING diodes (LEDs) based on GaN-based, blue-spectrum chips coated with yellow and red phosphors have become popular for applications in general lighting, display, and communication [1]. Because a single LED only has limited power output, multichip LED modules using the chips-on-board (COB) technology have been the preferable solutions for high power operations, such as downlights and high bay lights [2]. However, low light extraction efficiency (LEE) of multichip LED modules has been an issue because of the total internal reflection (TIR) effect [3] from the top packaging surface of the module can reduce the emission of light rays and cause the trapped light rays to convert into heat. Previously, various approaches were attempted to improve the LEE by reducing the TIR, including nanorandom/microrandom surface structures [4], [5], phosphor structures [6], [7], photonic crystal structures [8], [9], surface plasma treatments [10]–[12], and microlens arrays [13], [14]. Among the aforementioned methodologies, the nanosolution/microsolution could be costly due to the large emitting area of multichip LEDs at the packaging level. Some millimeter scale structures have been proposed and shown good performances with low manufacturing costs, such as conical or spherical patterned substrates [3], [15] and pyramid arrays substrates [16], [17]. Another popular structure is the V-grooves on the device substrate, which has been commonly used for light extraction or diffusion in light guide plates [18], [19]. These V-grooves can be fabricated by several low-cost processes, such as dicing [20], compression molding [21], and roll-to-roll stamping [18]. Dicing is a highly-efficient, convenient, and flexible process that could fit well for multichip LED modules. The whole process for dicing a set of multichip LEDs can be only about 100 s, which is shorter than that of the molding process (~500 s per cycle). Using V-shaped blades, the grooves can be processed on the surface of the chips or packages. For example, the DA series LED chip from CREE has the V-grooves on the SiC substrate to enhance the LEE [22].

The design of the grooves is a complex problem and ray tracing (RT) is one popular method [3], [15], [17], [23], which requires proper geometric optics approximations. Furthermore, the surface roughness of the substrate or package has been difficult to model. Previously, the experimental measurements have been commonly used to obtain the scattering properties of the rough surface as part of the RT tool to help solving the problem [24]. On the other hand, Liu *et al.* [25] has proposed a model for the blue LED chip by using the total integrated scattering theory. David has introduced a numerical model based on solving Maxwell's equations to describe the light scattering of a rough surface [25]. Compared with these methods, the finite-difference time-domain (FDTD) method has provided convenient and appropriate solutions for the light scattering effects on rough surfaces [26]. In our previous work, we have

Manuscript received August 24, 2016; revised October 25, 2016; accepted November 10, 2016. Date of publication November 22, 2016; date of current version December 24, 2016. This work was supported in part by the Natural Science Foundation of Guangdong Province, China, under Grant 2014A030312017, in part by the National Natural Science Foundation of China under Grant 51375177, Grant 51405161, and Grant U1401249. The review of this paper was arranged by Editor J. Huang. *(Corresponding author: Zongtao Li.)*

X. Ding, Y. Xie, and L. Lin are with the Department of Mechanical Engineering, University of California at Berkeley, Berkeley, CA 94720-5800 USA (e-mail: xrding@berkeley.edu; yingxixie@berkeley.edu; lwlin@berkeley.edu).

Y. Tang and J. Li are with the Key Laboratory of Surface Functional Structure Manufacturing of Guangdong Higher Education Institutes, South China University of Technology, Guangzhou 510641, China (e-mail: ytang@scut.edu.cn; qwd886me@qq.com).

Z. Li is with the Key Laboratory of Surface Functional Structure Manufacturing of Guangdong Higher Education Institutes, South China University of Technology, Guangzhou 510641, China, and also with Foshan Nationstar Optoelectronics Company, Ltd., Foshan 528000, China (e-mail: meztli@scut.edu.cn).

Color versions of one or more of the figures in this paper are available online at http://ieeexplore.ieee.org.

Digital Object Identifier 10.1109/TED.2016.2628788

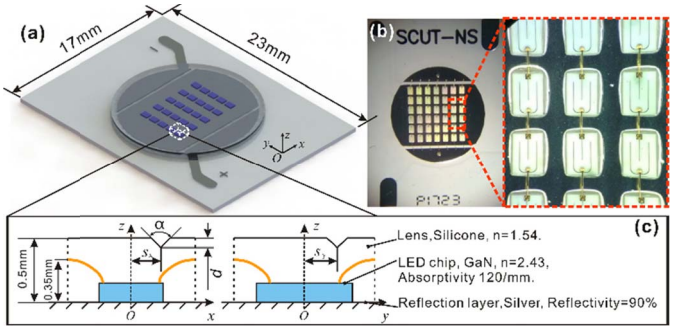

Fig. 1. (a) Schematic of the multichip LED module. (b) Photograph of a fabricated multichip LED module before applying the top packaging encapsulation material. (c) Simulation setups.

used this approach to effectively design micropatterned optical films [27] and phosphor particle layers [28].

Here, we propose to apply V-grooves on top of the multichip LED module packaging surface and utilize the Weierstrass-Mandlebrot fractal function to generate random roughness for the surfaces. The system is simulated by using an FDTD and RT combined method to investigate the light output efficiencies. It is found that our experimental results correspond well with the simulations with enhanced luminous efficiency by 9.6% (the simulation result of 13.7%) under an input current of 350 mA (5.8 W) when compared with the conventional multichip LED module without the V-grooves. Furthermore, we have utilized a fabricated multichip LED module with V-grooves in a downlight lamp for practical applications.

II. Experiment and Simulation Setups

We selected a commercial type P1723 multichip LED as the demonstration example in this paper, as shown in Fig. 1(a). The P1723 has the total dimension of 17×23 mm^2 and the top lens has the thickness of 0.5 mm to cover the bonding wires. A total of 42 commercial, GaN-based LED chips (20×30 mil^2 with the average dominant wavelength of 450 nm) were connected with six-series and seven-parallel wire bonding connections, as shown in Fig. 1(b). In general, three possible parameters should be considered for the design of the V-grooves on the top surface of the COB LEDs: the vertex angle, depth, and location. The cross-sectional view of a single LED unit in the module is shown in Fig. 1(c). α represents the vertex angle, d is the depth of the grooves, and s_x and s_y represent the distance between the groove and the center of each LED chip along the x- or y-direction, respectively. In consideration of the height of the golden wire, the maximum of d is set to 0.1 mm to prevent the golden wire from being damaged.

As shown in Fig. 2(a), light rays from the LED can pass through the top layer and emit outward in the escape region (green color). In terms of the location of the grooves, there are two possible regions to place the single V-groove. If the V-groove is placed within the escape cone zone, some light rays in the vertical direction could be reflected back and trapped inside the top lens area as shown in Fig. 2(b) to reduce the overall LEE. If the groove is placed outside the escape zone, some of the light rays, which originally would be reflected back and trapped due to the TIR effect [as shown

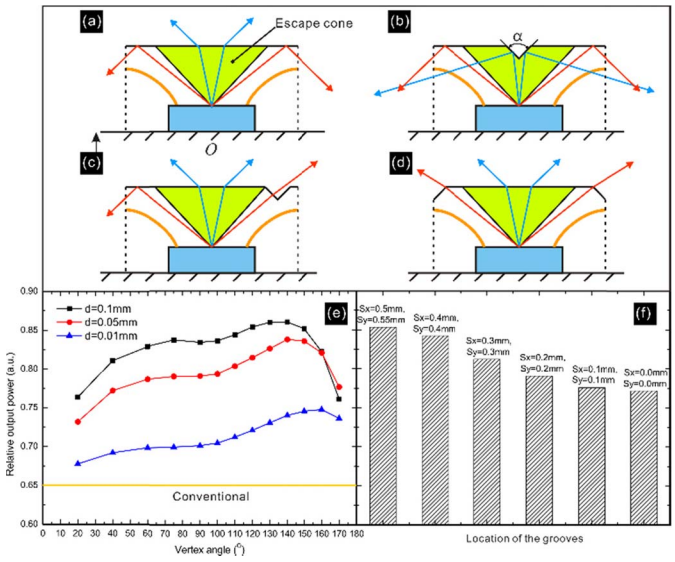

Fig. 2. (a) Cross-sectional view of a single LED with bonding wires (orange color) and the light ray escape cone (green color)—light rays will emit out of the LED module. Beyond the escape zone, light rays will reflect back to the LED module due to TIR. (b) V-groove is located inside the escape zone and some light rays will be reflected back to reduce the light emitting efficiency. (c) V-groove is placed outside the escape zone on the right side of the LED. Some of the originally light rays to be reflected back to the LED module (as illustrated in the left side of the LED) would be emitted out of the LED module due to the V-groove to increase the light emitting efficiency. (d) Best placement of a single V-groove in this paper is right at the intersection of two adjacent LED, such that both slopes of the V-groove can allow some light rays to emit outward to increase the light emitting efficiency. (e) and (f) Simulation results of relative output power versus vertex angles, depths, and locations of the grooves.

at the left side of Fig. 2(c)], will now emit outward at the left slope of V-groove [as shown at the right side of Fig. 2(c)]. Under the assumption that only one V-groove is used per LED, the best location of the V-groove is at the intersection of two adjacent chips, as shown in Fig. 2(d). This will allow both slopes [instead of only one slope in Fig. 2(c)] of the groove to redirect light rays outwards. The simulation results of relative output power versus locations proves the above analysis, as shown in Fig. 2(f). In terms of the vertex angle and depth of the groove, the best range is 120° to 150° with the depth of 0.1 mm according to Fig. 2(e). However, the large vertex angle will lead to a thick cutting blade, which is not cost-effective. Therefore, with the similar relative output power, we constructed V-grooves at the edge of each unit with a vertex angle of 120° and a depth of 0.1 mm.

Fig. 3 shows the packaging and dicing procedures of the multichip LEDs. A flattened lens mold was applied to package the module, as shown in Fig. 3(a) and (b). The surface of the mold was polished with a measured surface roughness of 0.06 μm (rms). Afterward, a high-speed dicing saw (Disco DAD322) with a maximum revolution speed of 40 000 r/min, and a maximum cutting speed of 500 mm/s was applied to fabricate the V-grooves on the top surface of the lens in Fig. 3(c). The dicing blade was made by coating boron nitride on the metal base with a thickness of 0.35 mm. Fig. 3(d) shows the optical photos by confocal laser microscope—Olympus OLS4000. The RMS surface roughness of the groove is estimated as 0.25 μm.

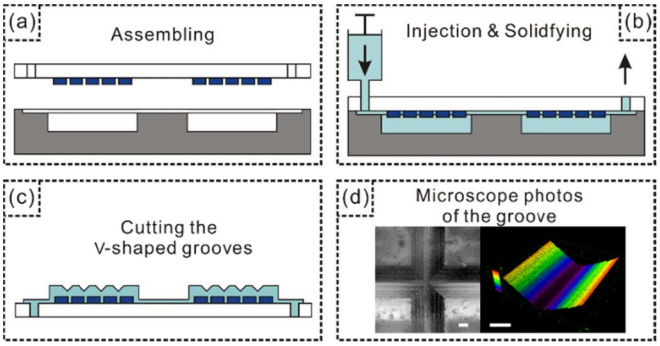

Fig. 3. Fabrication process of the multichip LED module. (d) Scale bar is 100 μm.

TABLE I
Parameters of the Fractal Model

D	L_0(μm)	L_s(μm)	γ	M	G
2.7	200	$4\text{x}10^{-6}$	1.5	10	0.005~0.045 (RMS 0.058~0.439μm)

If the rough surface is scale independent and random, the multiscale behavior can be modeled by the fractal theory and the Weierstrass–Mandlebrot fractal function is used in this paper to generate a surface with random roughness [29]

$$z(x,y) = L_0(G/L_0)^{D-2}((\ln\gamma)/M)^{0.5}\sum_{m=1}^{M}\sum_{n=0}^{n_{\max}}\gamma^{(D-3)n} \times\left[\cos\varphi_{m,n} - \cos\left(2\pi\gamma^n\sqrt{x^2+y^2} \times(\cos(\arctan(y/x) - \pi m/M))/L_0 + \varphi_{m,n}\right)\right] \quad (1)$$

where L_0 is the sample length, G is the fractal roughness, M is the number of superimposed ridges, $\varphi_{m,n}$ is a random phase, and D is the fractal dimension. The scaling parameter, γ, controls the density frequencies of the surface and $n_{\max}$ is expressed as

$$n_{\max} = \text{Int}\left[\frac{\log(L_0/L_s)}{\log\gamma}\right] \quad (2)$$

where the cutoff length L_s represents the minimum sample length. All above-mentioned parameters are defined in Table I [30], [31]. Surfaces of different roughness can be generated by changing the fractal roughness number G from 0.005 to 0.050, corresponding to rms of the surface of 0.058–0.439 μm.

The rough surface exhibits a variety of optical phenomena, including refraction, reflection, diffraction, and interference. The FDTD method was used to calculate the light scattering and transmittance properties. Fig. 4 shows the simulation setups in the numerical tool, FDTD solution from Lumerical. The perfectly matched layer boundary condition was applied to the top and bottom sides, and the Bloch boundary condition was applied to the side walls of the FDTD simulation region. The FDTD simulation region was set to 2-D and the plane wave with a dominant wavelength of 450 nm was set in the

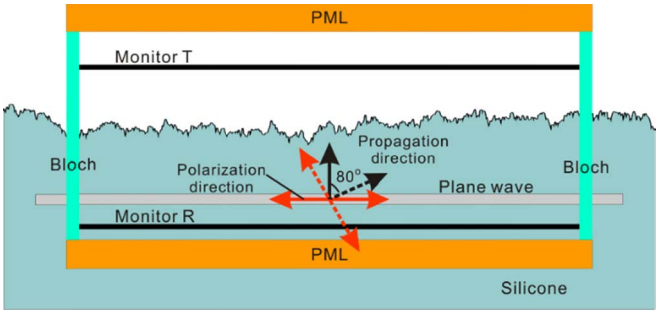

Fig. 4. FDTD simulation setups for a rough surface.

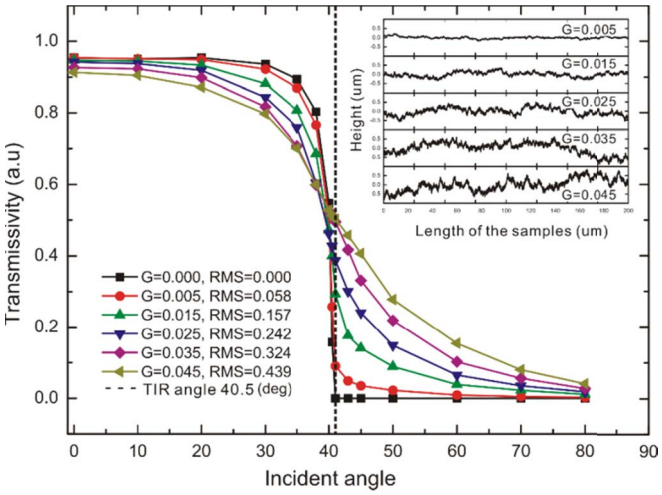

Fig. 5. Simulated transmittance versus different light incident angles from the proposed model. Inset: outlines of different surfaces.

side silicone. The propagation angle of the plane wave was varied from 0° (normal to the surface) to 80°. Two orthogonal polarizations were simulated for each propagation angle to realize unpolarized plane wave sources. A field monitor and a power monitor were set on the top of the surface to collect the propagated light rays. After that, the propagated light rays were transferred as a surface property by using the ABg scattering model as [32]

$$\text{BSDF}(\theta_i,\varphi_i,\theta_s,\varphi_s) = \frac{A}{B + |\vec{\beta} - \vec{\beta}_0|^g} \quad (3)$$

where BSDF is called the asymmetric bidirectional scattering distribution function, β_0 and β are the projection onto the surface of the unit vector in the specular direction and scattering direction, respectively, and A, B, and g are parameters that can be used to fit the formula to the FDTD data. Afterward, the simulation by RT method can be processed.

III. Results and Discussion

Fig. 5 shows the average transmittances of different surfaces versus the light incident angle. Here, two simulations with orthogonally polarized beams were conducted to simulate the unpolarized beam by calculating the average value of each polarized beam. The detailed method can be found in Lumerical's knowledge base [33]. If the light incident angle

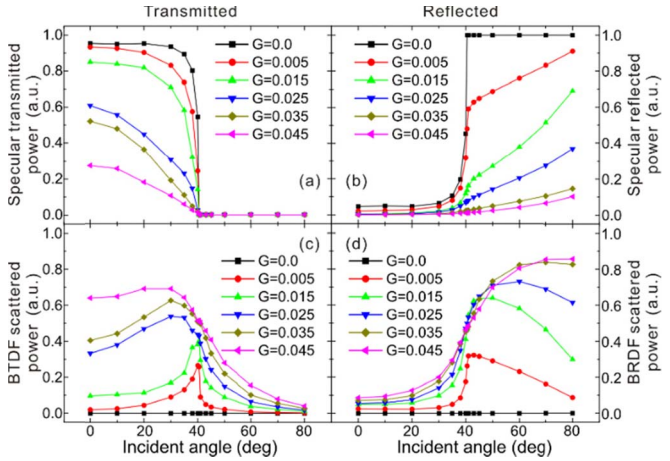

Fig. 6. (a) Specular transmitted (top left), (b) specular reflected (top right), (c) scattered BTDF, and (d) scattered BRDF power versus different light incident angles.

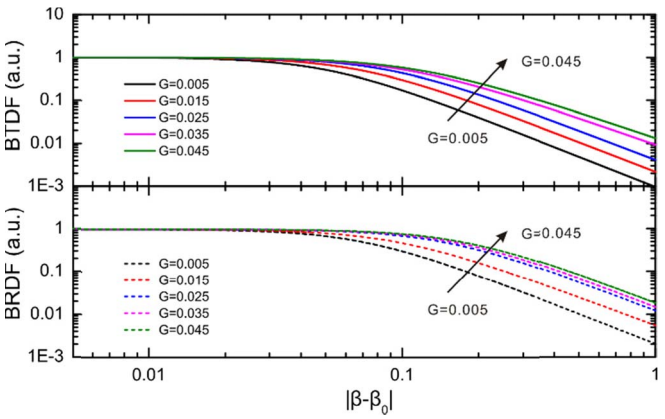

Fig. 7. Fitted BTDF and BRDF curves with the ABg model.

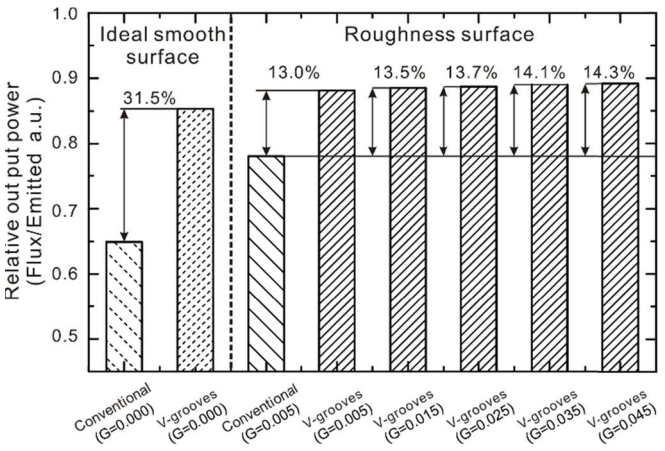

Fig. 8. Enhancement of the output power for surfaces with different roughness configurations. Left: surfaces are ideally flat without any roughness for the LED modules without and with the V-grooves. Right: flat regions of the LED module has G of 0.005 as measured in experiment. The surfaces of the slopes of the V-grooves have roughness from $G = 0.005$ to $G = 0.045$.

is smaller than the critical angle, the transmittance decreases as the roughness increases. If the incident angle is larger than the critical angle, the transmittance increases as the roughness increases. As such, the rough surface is helpful for the emission of large angle incident rays. The inset in Fig. 4 shows the outlines of different surfaces with calculated corresponding rms values. It is noted that our measured surface roughness in the flat area has rms of 0.06 μm, which corresponds to a G value of 0.005; while the slope of the V-grooves has rms of 0.25 μm, which corresponds to a G value of 0.025. The reflectance can be calculated by subtracting the transmittance from total energy.

Both of the transmitted and reflected light rays contain two parts of energy, specular, and scattered energy. The scattered energy in the specular direction is defined as the average energy of two adjacent orders, which are on the left and right of the specular direction. Thus, the specular transmittance and the specular reflectance can be obtained by subtracting the scattered energy in the specular direction from the specular energy. The specular and scattered energy with different light incident angles are simulated and shown in Fig. 6. It is found that the specular power increases [Fig. 6(a) and (b)] and scattered bidirectional transmittance distribution function (BTDF) and BRDF power decreases [Fig. 6(c) and (d)], respectively, as the surface roughness increases. Intuitively, the reason comes from the fact that rough surface can diffuse the specular light [34]. Furthermore, for the transmitted region in Fig. 6(a) (incident angle smaller than 40.5°), the specular energy decreases as the light incident angle increases. When the incident angle is larger than the critical angle, the specularly transmitted light disappears due to TIR. However, there are still scattered light rays that can transmit through the surface when the incident angle is larger than 40.5°, for rough surfaces.

The scattering distributions of surface with different roughness are simulated and shown in Fig. 7. The normalized scattering distributions of BTDF and BRDF are fitted by the ABg scattering model in (3). The BSDF parameters including the specular transmittance and reflectance, scattered transmittance and reflectance can be used in the simulations of the whole multichip LED module. The surface property of $G = 0.005$ has been applied on the flattened surface (measured experimentally). On the other hand, the surface properties from $G = 0.005$ to $G = 0.045$ have been applied on the V-groove surfaces with results shown in Fig. 8. It is noted that G value of 0.025 or rms of 0.242 μm matched closely with the measured rms of 0.25 μm [Fig. 3(d)].

If the surfaces were ultra smooth, it is found that the multichip LED module using the proposed V-grooves will have 31.5% higher power outputs (the left part in Fig. 8) as compared with that of the flattened LED module. In more realistic situation, surface roughness is applied (the right part of Fig. 8) and several results have been observed. First, the relative output power of the multichip LED module without the V-groove has enhanced relative output power from 0.65 to 0.78. Second, the V-groove texture can further increase the relative output power from 0.88 to 0.89 as the surface roughness increases from $G = 0.005$ to $G = 0.045$. It is noted that V-grooves with high surface roughness is more desirable from these results. However, since the total surface

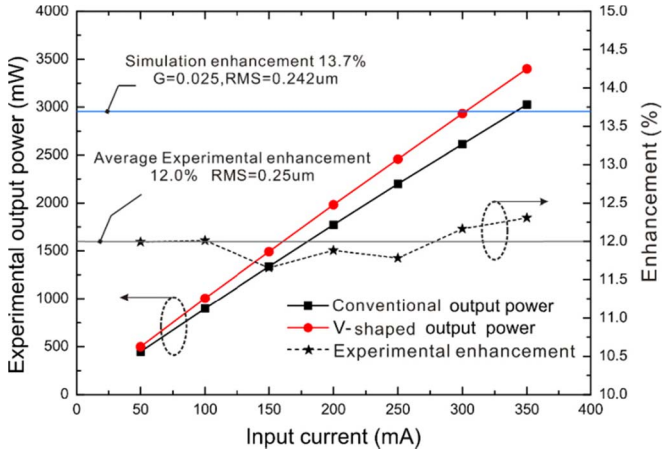

Fig. 9. Experimental output power of the multichip LED module with respect to the input current before (black) and after the proposed V-groove texture (red) and their power enhancements.

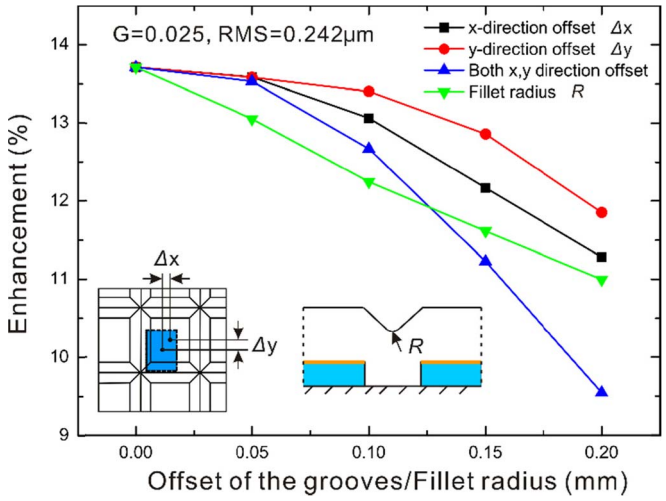

Fig. 10. Output power enhancements with respect to the various offsets of the grooves: in the *x*-direction (black), the *y*-direction (red), and both the *x*- and *y*-directions (blue). Output power enhancements with respect to the various fillet radius of the grooves (green).

areas of V-grooves are relatively small as compared with the whole top surface areas of the multichip LED module, these enhancements are relatively small.

Experimentally, the multichip LED module has been fabricated and its optical properties have been measured before and after adding the V-grooves textures on the top surface. As the applied current increases from 50 to 350 mA, the output power increases linearly, as shown in Fig. 9. The average output power enhancement without and with the V-groove is 12%, which is 1.7% lower than the simulation results. The discrepancy comes from: 1) the simulation model assumes that the surface roughness is isotropous but the grooves are fabricated by the dicing process and the morphology of the surface is likely anisotropic along the dicing directions and 2) the simulation model neglects the effects of electrodes and bonding wires. These could result in overestimations in the output power simulations. Furthermore, the dicing process could have offset and shape errors. Fig. 10 shows the simulations results of the output optical power enhancements

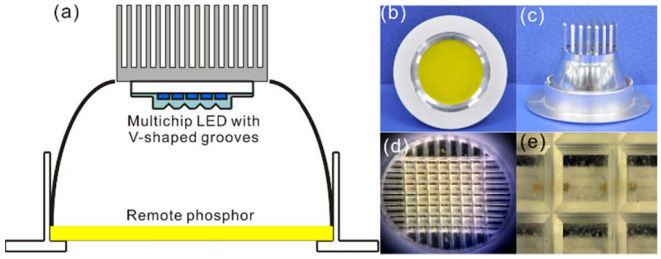

Fig. 11. (a) Illustrations of the remote phosphor downlight. (b) Bottom view. (c) Side view. (d) Photograph of the axonometric view. (e) Microscope photograph of the V-grooves.

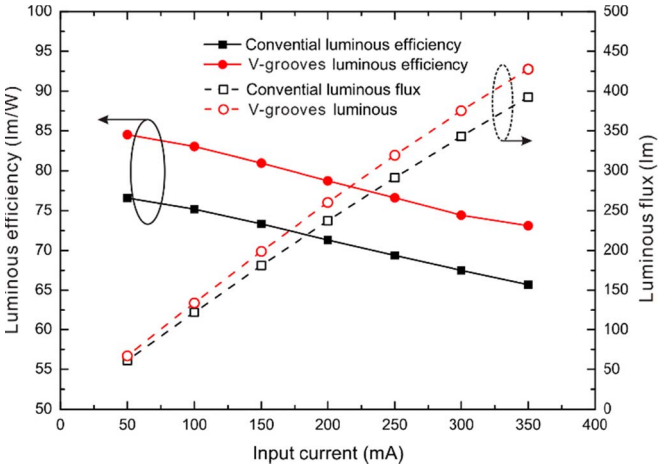

Fig. 12. Experimental output power and luminous of the downlight with and without V-shaped grooves.

versus V-groove offset along the *x*-direction (black line), *y*-direction (red line) and both the *x*- and *y*-directions (blue line). In general, the enhancements decrease as the offset errors increase while *y*-directional offset has the least impact on the overall enhancement efficiencies and the combined *x*- and *y*-directional offset has the most reductions on the overall enhancement efficiencies. The shape errors include vertex angle error and fillet radius error. The former one lightly impacts the enhancement efficiency. When the vertex angle is within $120° \pm 5°$, the error of the enhancement is just within $\pm 0.6\%$. However, the fillet radius error, which comes from the wear of the blade, impacts the enhancement efficiency a lot, as shown in Fig. 10 (green line). It has linear reductions on the overall enhancement efficiencies with the slope of -13.74%/mm.

The fabricated multichip LED module with V-grooves has been utilized in a remote phosphor downlight application, as shown in Fig. 11. The luminous efficiency and the flux have been shown in Fig. 12. Under an input current of 350 mA (5.8W), the luminous flux can reach 427.6 lm with the luminous efficiency of 73.1 lm/W. The average enhancements of the multichip LED module with V-grooves for the luminous efficiency and flux are about 9.6%, respectively, higher than those without V-grooves. The decrease of the overall enhancement as compared with the multichip LED module should come from the different flux distributions on the remote phosphor for the multichip LED system.

IV. Conclusion

This paper has demonstrated both analytically and experimentally that applying V-groove textures on the top surface of the multichip LED module can enhance the light output power. It is noted that several constraints have been applied in this paper, such as single V-groove texture and geometry, the placement location, material, and thickness of the lens layer. Further studies can include or change these parameters to correspond better with practical manufacturing conditions. On the other hand, the typical fabrication process for the multichip LED modules uses low-cost dispensing process for the encapsulant instead of the molding process. Therefore, the top surface is a convex shape and the depth of the grooves in the peripheral could be shallower than those in the central regions. These factors will need to be put into the considerations in design and simulation processes. Nevertheless, the approach of dicing grooves on the multichip LED top surface is expected to provide higher LEE and is a convenient and low-cost method to enhance the output power for multichip LED modules.

References

[1] J. Cho, E. F. Schubert, and J. K. Kim, "Efficiency droop in light-emitting diodes: Challenges and countermeasures," *Laser Photon. Rev.*, vol. 7, no. 3, pp. 408–421, Jan. 2013.

[2] S. P. Ying and W. B. Shen, "Thermal analysis of high-power multichip COB light-emitting diodes with different chip sizes," *IEEE Trans. Electron Devices*, vol. 62, no. 3, pp. 896–901, Mar. 2015.

[3] Z. Huai, Z. Zhili, W. Yiman, L. Lang, L. Sheng, and L. Xiaobing, "Effect of patterned substrate on light extraction efficiency of chip-on-board packaging LEDs," in *Proc. IEEE 64th Electron. Compon. Technol. Conf. (ECTC)*, May 2014, pp. 1876–1879.

[4] T. Son, K.-Y. Jung, and J. Park, "Enhancement of the light extraction of GaN-based green light emitting diodes via nanohybrid structures," *Current Appl. Phys.*, vol. 13, no. 6, pp. 1042–1045, Mar. 2013.

[5] P. Mao, A. K. Mahapatra, J. Chen, M. Chen, G. Wang, and M. Han, "Fabrication of polystyrene/ZnO micronano hierarchical structure applied for light extraction of light-emitting devices," *ACS Appl. Mater. Interfaces*, vol. 7, no. 34, pp. 19179–19188, Aug. 2015.

[6] H. Xiao, Y. Lu, C. Chai, Y. Wang, and Z. Chen, "Red-phosphor-dot-doped array in mirror-surface substrate light-emitting diodes," *J. Display Technol.*, vol. 12, no. 8, pp. 873–877, Mar. 2016.

[7] Z.-T. Li, Y. Tang, Z.-Y. Liu, Y.-E. Tan, and B.-M. Zhu, "Detailed study on pulse-sprayed conformal phosphor configurations for LEDs," *J. Display Technol.*, vol. 9, no. 6, pp. 433–440, 2013.

[8] A. Zhen *et al.*, "Embeded photonic crystal at the interface of p-GaN and AG reflector to improve light extraction of GaN-based flip-chip light-emitting diode," *Appl. Phys. Lett.*, vol. 105, no. 25, p. 251103, Dec. 2014.

[9] D. Pudis *et al.*, "Effect of 2D photonic structure patterned in the LED surface on emission properties," *Appl. Surf. Sci.*, vol. 269, pp. 161–165, Oct. 2013.

[10] S. Butun, S. Tongay, and K. Aydin, "Enhanced light emission from large-area monolayer MoS_2 using plasmonic nanodisc arrays," *Nano Lett.*, vol. 15, no. 4, pp. 2700–2704, Apr. 2015.

[11] C.-Y. Cho *et al.*, "Surface plasmon-enhanced light-emitting diodes with silver nanoparticles and SiO_2 nano-disks embedded in *p*-GaN," *Appl. Phys. Lett.*, vol. 99, no. 4, p. 041107, Jul. 2011.

[12] J.-H. Yun *et al.*, "Enhanced optical properties of nanopillar light-emitting diodes by coupling localized surface plasmon of Ag/SiO_2 nanoparticles," *Appl. Phys. Exp.*, vol. 8, no. 9, p. 092002, Aug. 2015.

[13] P. Zhu, G. Liu, J. Zhang, and N. Tansu, "FDTD analysis on extraction efficiency of GaN light-emitting diodes with microsphere arrays," *J. Display Technol.*, vol. 9, no. 5, pp. 317–323, May 2013.

[14] P. Zhu, G. Liu, J. Zhang, and N. Tansu, "Light extraction enhancement of bulk GaN lightemitting diode with hemisphere-cones-hybrid surface," *J. Display Technol.*, vol. 9, no. 5, pp. 317–323, Jul. 2013.

[15] Z.-T. Li, Q.-H. Wang, Y. Tang, C. Li, X.-R. Ding, and Z.-H. He, "Light extraction improvement for LED COB devices by introducing a patterned leadframe substrate configuration," *IEEE Trans. Electron Devices*, vol. 60, no. 4, pp. 1397–1403, Apr. 2013.

[16] P. Kumar, S. Y. Son, R. Singh, K. Balasundaram, J. Lee, and R. Singh, "Analytical treatment of light extraction from textured surfaces using classical ray optics," *Opt. Commun.*, vol. 284, no. 20, pp. 4874–4878, Jul. 2011.

[17] C.-S. Wang and J.-W. Pan, "Light extraction efficiency of GaN-based LED with pyramid texture by using ray path analysis," *Opt. Exp.*, vol. 20, no. 5, p. A630, Sep. 2012.

[18] C.-W. Liu, C.-H. Lee, C.-J. Ting, T.-H. Lin, and S.-C. Lin, "Roll-to-roll process-based sub-wavelength grating for a color-separation backlight," *J. Display Technol.*, vol. 9, no. 7, pp. 561–564, Jul. 2013.

[19] C.-F. Chen and S.-H. Kuo, "A highly directional light guide plate based on V-groove microstructure cell," *J. Display Technol.*, vol. 10, no. 12, pp. 1030–1035, Dec. 2014.

[20] J. Xie, Y. Zhuo, and T. W. Tan, "Experimental study on fabrication and evaluation of micro pyramid-structured silicon surface using a V-tip of diamond grinding wheel," *Precis. Eng.*, vol. 35, no. 1, pp. 173–182, Sep. 2011.

[21] P. He, L. Li, H. Li, J. Yu, L. J. Lee, and Y. Y. Allen, "Compression molding of glass freeform optics using diamond machined silicon mold," *Manuf. Lett.*, vol. 2, no. 2, pp. 17–20, Jan. 2014.

[22] P. Mao *et al.*, "Dual enhancement of light extraction efficiency of flip-chip light-emitting diodes with multiple beveled SiC surface and porous ZnO nanoparticle layer coating," *Nanotechnol*, vol. 26, no. 18, p. 185201, Apr. 2015.

[23] C. C. Chin, C. L. Wu, S. H. Tseng, C. Y. Chen, Y. L. Li, and D. W. Huang, "Photoinitiated polymerization for active packaging of light-emitting diodes," *IEEE Photon. J.*, vol. 5, no. 2, p. 2500110, Mar. 2013.

[24] N. Yan, T. Baar, M. O. Segovia, and J. Allebach, "Fitting analytical BRDF models to low-resolution measurements of light scattered from relief printing samples," *Electron. Imag.*, vol. 2016, no. 9, pp. 1–6, Feb. 2016.

[25] Z. Liu, K. Wang, X. Luo, and S. Liu, "Precise optical modeling of blue light-emitting diodes by Monte Carlo ray-tracing," *Opt. Exp.*, vol. 18, no. 9, pp. 9398–9412, Apr. 2010.

[26] L. Kuang and Y. Q. Jin, "Bistatic scattering from a three-dimensional object over a randomly rough surface using the FDTD algorithm," *IEEE Trans. Antennas Propag.*, vol. 55, no. 8, pp. 2302–2312, Aug. 2007.

[27] X. Ding, J. Li, Q. Chen, Y. Tang, Z. Li, and B. Yu, "Improving LED CCT uniformity using micropatterned films optimized by combining ray tracing and FDTD methods," *Opt. Exp.*, vol. 23, no. 3, pp. A180–A191, Feb. 2015.

[28] L. Jia-Sheng *et al.*, "A detailed study on phosphor-converted light-emitting diodes with multi-phosphor configuration using the finite-difference time-domain and ray-tracing methods," *IEEE J. Quantum Electron.*, vol. 51, no. 10, pp. 1–10, Aug. 2015.

[29] B. Chatterjee and P. Sahoo, "Finite element based contact analysis of fractal surfaces—Effect of varying elastic modulus," *Proc. Eng.*, vol. 90, pp. 116–122, Dec. 2014.

[30] W. Yan and K. Komvopoulos, "Contact analysis of elastic-plastic fractal surfaces," *J. Appl. Phys.*, vol. 84, no. 7, pp. 3617–3624, Jun. 1998.

[31] B. Chatterjee and P. Sahoo, "Finite element based contact analysis of fractal surfaces-effect of varying elastic modulus," *Proc. Eng.*, vol. 90, pp. 116–122, Dec. 2014.

[32] E. R. Freniere, G. G. Gregory, and R. C. Chase, "Interactive software for optomechanical modeling," *Proc. SPIE*, vol. 3130, pp. 128–133, Sep. 1997.

[33] Lumerical, *Knoledge Base for Unpolarized Beam*. [Online]. Available: https://kb.lumerical.com/en/index.html?ref_sim_obj_fdtd_coherence_unpolarized_beam.html

[34] J. E. Harvey, S. Schröder, N. Choi, and A. Duparré, "Total integrated scatter from surfaces with arbitrary roughness, correlation widths, and incident angles," *Opt. Eng.*, vol. 51, no. 1, pp. 013402-1–013402-11, Jan. 2012.

Xinrui Ding was born in Zhengzhou, China, in 1987. He received the Ph.D. degree in mechanical engineering with a Minor in Microelectronics Manufacture Engineering degree from the South China University of Technology, Guangzhou, China, in 2015.

He is currently a Post-Doctoral Researcher with the Mechanical Engineering Department, University of California at Berkeley, Berkeley, CA, USA. His current research interests include the LED packaging, optical designing, lighting quality, and reliability.

Yong Tang received the Ph.D. degree in mechanical engineering from the South China University of Technology, Guangzhou, China, in 1994.

He is currently a Professor with the School of Mechanical and Automotive Engineering, South China University of Technology, and the Director of the Key Laboratory of Surface Functional Structure Manufacturing of Guangdong, Higher Education Institutes, South China University of Technology. His current research interests include surface properties in clean energy and its high efficient usage, especially in energy saving solid-state lighting.

Zongtao Li received the Ph.D. degree in mechanical engineering with a Minor in Microelectronics Manufacture Engineering degree from the South China University of Technology, Guangzhou, China, in 2013.

He is currently with the Key Laboratory of Surface Functional Structure Manufacturing of Guangdong, Higher Education Institutes, South China University of Technology, and the Optoelectronics Engineering Technology Research and Development Center, Foshan NationStar Optoelectronics Company, Ltd., Foshan, China. His current research interests include packaging of high-power LEDs, lighting quality, and device reliability.

Jiasheng Li received the B.E. degree in mechanical engineering and automation from the South China University of Technology, Guangzhou, China, in 2014, where he is currently pursuing the master's degree with the Key Laboratory of Surface Functional Structure Manufacturing of Guangdong, Higher Education Institutes.

His current research interests include the LED packaging and lighting quality.

Yingxi Xie received the B.E. degree in mechanical engineering and automation from the South China University of Technology, Guangzhou, China, in 2011, where he is currently pursuing the Ph.D. degree with the Key Laboratory of Surface Functional Structure Manufacturing of Guangdong, Higher Education Institutes.

His current research interests include the LED packaging, MEMS, and supercapacitors.

Liwei Lin received the B.S. degree in power mechanical engineering from the National Tsing Hua University, Hsinchu, Taiwan, in 1986, and the M.S. and Ph.D. degrees in mechanical engineering from the University of California at Berkeley, Berkeley, CA, USA, in 1991 and 1993, respectively.

He currently serves as a Chancellor's Professor with the Department of Mechanical Engineering, University of California at Berkeley, and the Co-Director of the Berkeley Sensor and Actuator Center. His current research interests include microelectromechanical systems, nanoelectromechanical systems, nanotechnology, and microelectronics.